

Supplemental figure legends

Figure S1

Frequency distribution charts showing individual segment caliber changes in response to acetylcholine in **(a)** third and **(b)** fourth branching order vessels. The control group had a relatively high frequency of third and fourth branching order arterial vessels showing localized segmental vasoconstriction (ID constriction >5% of baseline). The frequency of abnormal vasoconstriction with acetylcholine in the control group was about 8- and 4-fold for the third and fourth branching order, respectively, as compared with the combined group (third order: control 49% vs. combined 6% vs. sheet-only 22% vs. OM-only 25%; fourth order: control 18% vs. combined 4% vs. sheet-only 13% vs. OM-only 17%).

Supplemental Materials and Methods

Construction of Cell-sheets

Skeletal myoblasts were isolated from tibialis anterior muscle tissues of 3-week-old male wild-type or GFP transgenic Lewis rats as appropriate, and cultured as previously described.¹ In brief, when the cells became approximately 70% confluent after 4 days of cultivation in Dulbecco's modified Eagle Medium (DMEM) (Gibco) with 20% fetal bovine serum (Sigma-Aldrich), they were transferred to 35-mm temperature-responsive culture dishes (UpCell, Cellseed, Tokyo, Japan) and incubated at 37°C, with the cell number adjusted to 3.0×10^6 per dish. After 24 hours, the cells were induced to spontaneously detach by cooling at 20°C for 30 minutes, which yielded a scaffold-free sheet-shaped monolayer of skeletal myoblasts for use as a graft.

Establishment of Chronic Myocardial Infarction Rat Model

Two hundred female Lewis rats (180-200 g, Charles River) underwent left coronary artery ligation as previously described.¹ The rats were anaesthetized by inhalation of isoflurane (2%, 0.2 mL/min), intubated, and placed on a respirator during surgery to maintain ventilation. The carrier gas for isoflurane is oxygen. The adequacy of anaesthesia was monitored by electrocardiography and pulse rate. Two weeks after left coronary artery ligation, transthoracic echocardiography was performed to validate the extent of myocardial infarction (MI). We aimed to create a widespread MI model, thus rats with a small extent of wall motion abnormality with ejection fraction greater than 45% were excluded (**Figure 1**). The widespread chronic MI models were randomly divided into 4 treatment groups: 1) cell-sheet transplantation covered with omentum (OM)-flap (combined group), 2) cell-sheet transplantation (sheet-only group), 3) OM-flap (OM-only group), and 4) sham operation

(control group) (**Figure 1**). In the sheet-only group, a five-layered cell-sheet was placed on the area and spread manually to cover both infarct and border areas. In the OM-only group, a small upper midline laparotomy was performed to manipulate the OM tissue. After making a small hole in the diaphragm, the pedicle OM-flap was then pulled from the peritoneal space to the pleural cavity using a transdiaphragmatic approach and wrapped directly onto the epicardium in the ischemic area. In the combined group, 5-layered cell-sheets were placed in a similar manner as in the sheet-only group, then covered with the harvested OM-flap.

Histological Analysis

Four weeks after the treatment, the rats were humanely killed by an intraperitoneal injection of pentobarbital (300 mg/kg) and heparin (150 U) for histological analysis of the heart tissue (n=11 for each group) (**Figure 1**). Anterior wall thickness was measured in at least 3 hematoxylin and eosin-stained sections of the middle portion of the LV, while Sirius red staining was performed to assess myocardial fibrosis in the peri-infarct region. The fibrotic region was calculated as the percentage of myocardial area. Data were obtained from 5 individual views of each heart. Periodic acid-Schiff staining was performed to examine the degree of cardiomyocyte hypertrophy. Myocyte size was determined by drawing point-to-point perpendicular lines across the cross-sectional area of the cell at the level of the nucleus. The results are expressed as the average diameter of 20 myocytes randomly selected from 5 fields of each ventricle. The images were examined by optical microscopy (Olympus, Tokyo, Japan) and quantitative morphometric analysis for each sample was performed using Metamorph software (Molecular Devices, Sunnyvale, California, US).

RNA Extraction and Quantitative Reverse-transcription Polymerase Chain Reaction

The myocardial gene expressions related to angiogenesis, vessel maturation, and anti-inflammation at 3 days after the treatment were assessed by quantitative reverse transcription PCR (**Figure 2**). Total RNA was extracted from the peri-infarct myocardium using an RNeasy mini kit (Qiagen GmbH, Hilden, Germany), according to the manufacturer's instructions. For each sample, 1 µg of total RNA was converted to cDNA with Omniscript RT (Qiagen) and analyzed with a PCR array (Qiagen-SABiosciences) and Applied Biosystems® ViiA™ 7 real-time PCR system (Life Technologies Corporation). Data were normalized to β-actin expression level. Relative gene expression was determined using the $\Delta\Delta CT$ method.

Immunohistochemistry

Endothelial cells were labeled with rat monoclonal anti-CD31 antibody (Abcam, Cambridge, UK 1:50), while pericytes were labeled with mouse monoclonal anti-α-SMA antibody (DAKO, Glostrup, Danmark 1:50) and visualized by corresponding secondary antibodies (Alexafluor 488 or Alexafluor555; Alexafluor 647 Molecular Probes, Eugene, OR), then counterstained with Hoechst 33342 (Dojindo, Kumamoto, Japan). Vessel density and maturity were quantified as the number of CD31 positive vessels and CD31/α-SMA double-positive vessels per mm², respectively. A maturation index was calculated as the percentage of CD31/α-SMA double-positive vessels to total vessel number. Vessels positive for CD31 but negative for lectin were regarded as functionally immature vessels undergoing regression or that had lost patency.²

Evaluation of Mature Vessels with Patent Endothelial Layers

Mature vessels with patent endothelial layers were assessed by injection of 500 µl of Alexa Fluor 568 conjugate-labeled esculentum lectin (500 µg in 500 uL in 0.9% NaCl; GS-IB4,

Molecular Probes, Eugene, OR), which binds uniformly and rapidly to the luminal surface of endothelium and thus labels patent blood vessels, into a tail vein 30 minutes before tissue sampling.² Myocardial tissues were then removed, immersed in fixative for 1 hour in 4% paraformaldehyde, rinsed several times with PBS, infiltrated with 30% sucrose, frozen in OCT compound, and processed for immunohistochemistry.

Vessel Recruitment in the Transplanted Cell-sheets

To evaluate the angiogenic effect of the OM-flap in the transplanted area, we serially assessed the number of functional blood vessels with patent endothelial layers (CD31/lectin double-positive cells) in the transplanted area of the sheet-only and combined groups at 3, 7 and 28 days after each treatment (n=6 for each group and each time point) (**Figure 3**).

Vessel Remodeling and Maturation in Peri-infarct Myocardium

We serially assessed neovascular vessel maturity in peri-infarct areas at 3 (n=6 for each group) and 28 days (n=11 for each group) after treatment (**Figure 4**). Vessel density and structural maturity were quantified as the number of CD31 positive and CD31/ α -smooth muscle actin (SMA) double-positive vessels per mm², respectively. A maturation index was calculated as the percentage of CD31/ α -SMA double-positive vessels to total vessel number.

Synchrotron radiation microangiography

To evaluate the effects of each treatment on microcirculation physiology in terms of relative dilatory responses to acetylcholine and dobutamine hydrochloride in the resistance vessels, synchrotron radiation microangiography was performed after 3 weeks after the treatment (control: n=11, combined: n=11, cell-sheet: n=5, OM: n=6) at SPring-8, Japan Synchrotron

Radiation Research Institute, Hyogo, Japan with approval from the Animal Experiment Review Committee in accordance with the guidelines of the Physiological Society of Japan, as previously described (**Figure 4**).³ In brief, under sodium pentobarbital anesthesia (50 mg/kg i.p.), examined rats were intubated and artificially ventilated (Shinano, Tokyo, Japan; 40% oxygen), then the right carotid artery was cannulated with a radiopaque 20-gauge BD Angiocath catheter (Becton Dickinson, Inc., Sandy, Utah, USA), placing the tip at the entrance of the aortic valve. Each rat was then placed in line with the horizontal X-ray beam and SATICON detector system (Hitachi Denshi Techno-system, Ltd., Tokyo, Japan and Hamamatsu Photonics, Shizuoka, Japan). Iodinated contrast medium (Iomeron 350; Bracco-Eisai Co. Ltd, Tokyo, Japan) was injected intrarterially as a bolus (0.3-0.5 ml at 0.4 ml/s) into the aorta using a clinical autoinjector (Nemoto Kyorindo, Tokyo, Japan) at the start of image recording scanning. At least 10 minutes was allowed for renal clearance of the contrast between imaging scans. Following a baseline recording, an endothelium-dependent vasodilatory response was recorded as an angiogram series at the end of a 5-minute infusion of acetylcholine (5 µg/kg/min). A third image series was recorded after a 5-minute infusion of dobutamine hydrochloride (8 µg/kg/min) to assess the ability to maintain perfusion of the infarcted region during increased heart work.

Assessment of Vessel ID during Synchrotron Angiography

Quantitative analysis of vessel internal diameter (ID) was based on measurements from the middle of discrete vessel segments in individual cine-radiogram frames using Image-J (v1.41, NIH, Bethesda, USA) for individual rats during each treatment period. Arterial vessels were categorized according to their branching order.³ The results for vessel ID in each rat during drug infusions are expressed as percentage changes from baseline (Δ), to account for

differences in absolute baseline vessel ID among the groups.

Quantification of Segmental Vasoconstrictions during Synchrotron Angiography

The relative change in vessel caliber in response to vasoactive agents gives no indication of vessel number with calibers less than the individual's mean change. Therefore, the number of abnormal vasoconstrictions during treatment periods was quantified. Localized segmental vasoconstrictions were considered to be present when a vessel segment showed an ID constriction of >5% of baseline vessel ID value.^{3,4}

PET measurements and data analysis

To evaluate the effects of each treatment on global and regional myocardial blood flow (MBF) and coronary flow reserve (CFR), ¹³N-ammonia PET measurements were serially performed 1 day before and 3 weeks after treatment (control: n=5, combined: n=8, cell-sheet: n=7, OM: n=7) (**Figure 5**). Rats were anesthetized with 2% isoflurane plus 100% oxygen and a cannula was inserted into the tail vein. PET data were acquired using a small animal PET device (Inveon PET/CT system, Siemens). Dynamic 10-minute PET measurements were started with an administration of ¹³N-NH₃ over 20 seconds (approximately 20 and 80 MBq for the rest and stress study, respectively).⁵ The stress study was performed 5 minutes after bolus injection of CGS-21680 (5 µg/kg), a selective adenosine A_{2A} agonist that induced coronary vasodilatation and increases in the MBF.

The PET data were reconstructed into 23 frames (12 fr × 5 s, 6 fr × 10 s, 4 fr × 30 s, 1 fr × 360 s) using the 3-dimensional ordered subset expectation maximization method followed by maximum a posteriori (3D-OSEM/MAP). Regions of interest were semi-automatically placed on the left ventricle myocardium and blood pooled inside the left and right ventricle, with

reference to the summed PET and CT images. MBF was calculated using the one-tissue compartment model developed by DeGrado et al. with PMOD software.⁶ Global and regional MBF (basal, mid, apical segments) were used for the evaluations.⁷ CFR was expressed as the ratio of MBF during stress to MBF at rest. Change in CFR was evaluated as the ratio of post-treatment to pre-treatment CFR. Normal male SD rats (n=6, 10-11 weeks old, BW: 369-429 g) were used for the validation study for quantitative PET measurements with a stress agent.

Assessment of Cardiac Function

The cardiac function was evaluated by echocardiography 2 and 4 weeks after each treatment (n=11 for each group) (**Figure 6**). Baseline measurements were made before each treatment. Transthoracic echocardiography was performed with using a SONOS 5500 (Philips Electronics, Tokyo, Japan) equipped with a 12-MHz annular array transducer under general anaesthesia induced and maintained by inhalation of isoflurane (2%, 0.2 mL/min) as mentioned above (**Figure 1**). The hearts were imaged in short-axis 2D views at the level of the papillary muscles, and the LV end-systolic and end-diastolic dimensions were determined. LV ejection fraction was calculated by Pombo's method.

LV pressure-volume loop analysis with cardiac catheterization was performed for each group as previously described.¹ In brief, a median sternotomy was performed and the LV apex was carefully dissected to minimize hemorrhaging. A MicroTip catheter transducer (SPR-671; Millar Instruments, Inc, Houston, Tex) and conductance catheter (Unique Medical Co, Tokyo, Japan) were then placed longitudinally into the left ventricle from the apex. LV pressure-volume relationships were determined by transiently compressing the inferior vena cava.

Exercise Tolerance

Eleven rats in each group were acclimated to a rodent activity wheel (MULTI-FUNCTIONAL ACTIVITY WHEEL, MK-770M, Muromachi, Tokyo, Japan) by running daily for 5 days. During the acclimation period, the round speed was increased from 5 to 10 rpm, with the exercise duration maintained at 20 minutes. On the day of tolerance testing, animals were placed on the activity wheel at round speeds of 4 or 8 rpm and allowed to exercise until fatigue. Fatigue was defined as the point at which the animal failed to keep pace with the activity wheel despite constant physical prodding for 1 minute. Running distance was used as an index of maximal capacity for exercise.

Communication Between Pedicle Omentum and Native Coronary Artery

Communication between the coronary arteries and branches of the gastroepiploic artery in the OM specimens was evaluated using 3 different methods in a different series of OM-only and combined group (n=12 for each group) (**Figure 7**).

Aortic Root Angiography using Barium Sulfate

We performed a postmortem angiography examination from the aortic root to verify antegrade flow from the OM into the heart (n=4 for each). In brief, a catheter with an internal diameter of 0.89 mm (COVIDIEN Ltd, Tokyo, Japan) was inserted from the right carotid artery into the aortic root, followed by systemic heparinization (1000 IU heparin). The rats were euthanized with an overdose of pentobarbital, then an incision was made in the right jugular vein and lactated Ringer's solution was manually perfused through the cannula for 5 minutes. Approximately 3 mL of a solution consisting of 70% weight/volume barium sulfate

suspended in 7% gelatin was then injected in a retrograde manner via the catheter using a programmed syringe pump. Angiograms were obtained with a angiographic system (MFX-80HK, Hitex) consisting of an open type 1- μ m microfocus X ray source (L9191, Hamamatsu Photonics) and a 50/100 mm (2"4") dual mode X-ray image intensifier (E5877JCD1-2N, Toshiba) set at 60 kV and 60 μ A.

Selective India Ink Perfusion via Celiac Artery

Next, we selectively injected India ink into the celiac artery to visually and histologically confirm vessel communication between the pedicle OM and native coronary artery (n=4 for each). The catheter was inserted via the abdominal aorta and its tip placed near the celiac artery, followed by systemic heparinization. The chest was reopened to expose the wrapped heart, taking care to avoid injuring the OM. The heart was harvested after perfusion fixation of the vasculature, as described above. We ligated the abdominal aorta just proximal from the tip of the catheter in advance and selectively injected India ink via the celiac artery into the heart, and then performed histological analysis.

Selective Perfusion via Aortic Root and Celiac Artery Using Two Different MICROFIL Colors

A catheter was inserted from the right carotid artery into the aortic root and another was inserted from the abdominal aorta into the celiac artery, followed by systemic heparinization (1000 IU heparin). After perfusion fixation, we ligated the abdominal aorta just proximal from the tip of the catheter. Approximately 3 mL of 2 different colors of MICROFIL solution (MICROFIL Silicone Rubber Injection Compounds, Flow Tech, Inc.) was injected in an antegrade manner into the celiac arterial trunk (MV-120 Blue) and a retrograde manner from

the aortic root into the coronary artery (MV-117 Orange). The solution was allowed to solidify for more than 30 minutes. The heart and OM were removed en bloc, and placed in 10% neutral buffered formalin for several days. The tissue was then cleared using sequential 24-hour incubations in 25% ethanol, 50% ethanol, 75% ethanol, 95% ethanol, 100% ethanol, and methylsalicylate, according to the manufacturer's instructions. Evidence of vessel communication between the native coronary artery and OM-flap was photographed in multiple planes using an Olympus DP70 camera attached to an Olympus SZX 12 stereo microscope (Olympus, Tokyo, Japan).

Creation of Surgically Joined Parabiotic Pairs Model

To further confirm whether the OM- and host myocardium-derived endothelial cells migrated toward the cell-sheet, we established two types of parabiotic pair models (n=4 for each) (**Figure 8**). To determine whether OM-derived endothelial cells migrated toward the cell-sheet, the parabiotic pairs model were established by producing wild-type MI model rats (recipient) to receive transplantation of wild-type oriented cell-sheets which was labeled with Cell Tracker TM Orange CMTMR (Invitrogen, Oregon, USA), followed by coverage with a pedicle OM derived from a transgenic ubiquitously expressing GFP rat (donor) and then surgically joining them. Similarly, to determine whether host myocardium-derived endothelial cells migrated toward the cell-sheet, we also established another parabiotic pairs model by producing GFP-transgenic MI model rats (recipient) to receive transplantation of wild-type oriented cell-sheets which was labeled with Cell Tracker TM Orange CMTMR, followed by coverage with a pedicle OM derived from a wild-type rat (donor) and then surgically joining them.

Parabiotic pair rats were anaesthetized by inhalation of isoflurane (2%, 0.2 mL/min) and

maintained for 72 hours under mechanical ventilation with a continuous infusion of 5% glucose (0.3 ml/h), then subjected to histological analyses.

In vitro Migration assay

To investigate cell migration in response to skeletal myoblast cells cultured in conditioned medium, a modified Boyden chamber migration assay was performed using an HTS FluoroBlok™ Multiwell Insert System (BD Falcon, NJ, USA) containing filters with a pore size of 8 µm. Briefly, human umbilical vein endothelial cells (HUVECs) (purchased from Lonza) were grown in EGM-2 culture medium (Lonza, Walkersville, USA). To visualize them, HUVECs were stained in advance with Cell Tracker TM Orange CMTMR (Invitrogen, Oregon, USA). A suspension of 5×10^4 HUVECs in HUVEC-cultured medium (350 µm) was applied to each upper chamber. The lower chamber was filled with 1.0 ml of concentrated skeletal myoblasts-cultured supernatant composed of DMEM with 20% fetal bovine serum (100% conditioned medium), 10-fold diluted conditioned medium (10% conditioned medium) or DMEM, and 20% fetal bovine serum (control group). After incubation at 37°C for 2 hours, the number of migrated cells was counted in 15 randomly chosen fields under 100×magnification using fluorescence microscopy (BIOREVO BZ-9000, KEYENCE, Osaka, Japan). Two replicate samples were used in each experiment, which were performed at least twice. Migrating cells were analyzed using a light microscope and reported as numbers of migrating cells per mm².

Statistical analysis

Data are expressed as the mean ± SEM unless otherwise stated. Student's t test (2 tailed) was used to compare 2 groups of independent samples. One-way and two-way ANOVA with

Bonferroni correction for repeated measures were performed to assess within and between group differences following the treatments. Following ANOVA, between group comparisons were made using a Student's t-test (2-tailed). Multiplicity in pairwise comparisons was corrected by the Bonferroni procedure. The Statistical Package Software System (SPSS v15, SPSS Inc, Chicago, USA) and JMP 9.0 (SAS Institute Inc, Cary, NC) were used for all analyses, with *P* values <0.05 deemed to indicate significance.

References

1. Sekiya N, Matsumiya G, Miyagawa S, Saito A, Shimizu T, Okano T, Kawaguchi N, Matsuura N, Sawa Y. Layered transplantation of myoblast sheets attenuates adverse cardiac remodeling of the infarcted heart. *J Thorac Cardiovasc Surg* 2009;**138**:985-993.
2. Mancuso MR, Davis R, Norberg SM, O'Brien S, Sennino B, Nakahara T, Yao VJ, Inai T, Brooks P, Freimark B, Shalinsky DR, Hu-Lowe DD, McDonald DM. Rapid vascular regrowth in tumors after reversal of VEGF inhibition. *J Clin Invest* 2006;**116**:2610-2621.
3. Jenkins MJ, Edgley AJ, Sonobe T, Umetani K, Schwenke DO, Fujii Y, Brown RD, Kelly DJ, Shirai M, Pearson JT. Dynamic synchrotron imaging of diabetic rat coronary microcirculation in vivo. *Arterioscler Thromb Vasc Biol* 2012;**32**:370-377.
4. Ludmer PL, Selwyn AP, Shook TL, Wayne RR, Mudge GH, Alexander RW, Ganz P. Paradoxical vasoconstriction induced by acetylcholine in atherosclerotic coronary arteries. *N Engl J Med* 1986;**315**:1046-1051
5. Croteau E, Bénard F, Bentourkia M, Rousseau J, Paquette M, Lecomte R. Quantitative myocardial perfusion and coronary reserve in rats with ¹³N-ammonia and small animal PET: impact of anesthesia and pharmacologic stress agents. *J Nucl Med* 2004;**45**:1924-1930.
6. DeGrado TR, Hanson MW, Turkington TG, DeLong DM, Brezinski DA, Vallée JP, Hedlund LW, Zhang J, Cobb F, Sullivan MJ, Coleman RE. Estimation of myocardial blood flow for longitudinal studies with ¹³N-labeled ammonia and positron emission tomography. *Med J Nucl Cardiol* 1996;**3**:494-507.
7. Cerqueira MD, Weissman NJ, Dilsizian V, Jacobs AK, Kaul S, Laskey WK, Pennell DJ, Rumberger JA, Ryan T, Verani MS; American Heart Association Writing Group on Myocardial Segmentation and Registration for Cardiac Imaging. Standardized myocardial

Kainuma S. et al. Cell-sheets Therapy Combined with Omentum flap - 16 -

segmentation and nomenclature for tomographic imaging of the heart. A statement for healthcare professionals from the Cardiac Imaging Committee of the Council on Clinical Cardiology of the American Heart Association. *Circulation* 2002;**29**;105:539-542.



Targeted Delivery of Adipocytokines Into the Heart by Induced Adipocyte Cell-Sheet Transplantation Yields Immune Tolerance and Functional Recovery in Autoimmune-Associated Myocarditis in Rats

Sokichi Kamata, MD, PhD; Shigeru Miyagawa, MD, PhD; Satsuki Fukushima, MD, PhD;
Yukiko Imanishi, PhD; Atsuhiko Saito, PhD; Norikazu Maeda, MD, PhD;
Iichiro Shimomura, MD, PhD; Yoshiki Sawa, MD, PhD

Background: Clinical prognosis is critically poor in fulminant myocarditis, while its initiation or progression is fated, in part, by T cell-mediated autoimmunity. Adiponectin (APN) and associated adipokines were shown to be immune tolerance inducers, although the clinically relevant delivery method into target pathologies is under debate. Whether the cell sheet-based delivery system of adipokines might induce immune tolerance and functional recovery in experimental autoimmune myocarditis (EAM) was tested.

Methods and Results: Scaffold-free-induced adipocyte cell-sheet (iACS) was generated by differentiating adipose tissue-derived syngeneic stromal vascular-fraction cells into adipocytes on temperature-responsive dishes. Rats with EAM underwent iACS implantation or sham operation. Supernatants of iACS contained a high level of APN and hepatocyte growth factor (HGF), and reduced proliferation of CD4-positive T cells in vitro. Immunohistolabelling showed that the iACS implantation elevated the levels of APN and HGF in the myocardium compared to the sham operation, which attenuated the immunological response by inhibiting CD68-positive macrophages and CD4-positive T-cells and activating Foxp3-positive regulatory T cells. Consequently, left ventricular ejection fraction was significantly greater after the iACS implantation than after the sham operation, in association with less collagen accumulation.

Conclusions: The targeted delivery of adipokines using tissue-engineered iACS ameliorated cardiac performance of the EAM rat model via effector T cell suppression and induction of immune tolerance. These findings might suggest a potential of this tissue-engineered drug delivery system in treating fulminant myocarditis in the clinical setting. (*Circ J* 2015; **79**: 169–179)

Key Words: Adiponectin; Inflammation; Myocarditis; Transplantation

Fulminant myocarditis often follows a rapidly deteriorating course, leading to severe cardiac dysfunction. Efficacy of fast-track immunoglobulin and steroid therapies has been reported,¹ but these treatments are not fully established. Although the pathogenesis of fulminant myocarditis is not fully understood, an autoimmune response against myocardial components has been suggested to play an important role in its progression, consequently leading to end-stage heart failure.^{1,2} Interferon (IFN) γ -producing T helper (Th)1 cells and interleukin (IL)17-producing Th17 cells are reported to be key regulators of the autoimmune response, as they ac-

tivate macrophages in the cardiac tissues to trigger inflammation and inhibit regulatory T cells.^{2,3} Strategies for ameliorating the immune response and/or augmenting immune tolerance are therefore under development for treating fulminant myocarditis.

Editorial p51

Fat tissue functions as a type of endocrine organ by secreting its produced cytokines and adipokines, which have pro-inflammatory and anti-inflammatory activities. Adiponectin

Received July 31, 2014; revised manuscript received September 13, 2014; accepted September 24, 2014; released online November 5, 2014 Time for primary review: 19 days

Department of Cardiovascular Surgery (S.K., S.M., S.F., Y.I., A.S., Y.S.), Department of Metabolic Medicine (N.M., I.S.), Osaka University Graduate School of Medicine, Suita, Japan

Mailing address: Yoshiki Sawa, MD, PhD, Department of Cardiovascular Surgery, Osaka University Graduate School of Medicine, 2-2 Yamadaoka, Suita 565-0871, Japan. E-mail: sawa-p@surg1.med.osaka-u.ac.jp

ISSN-1346-9843 doi:10.1253/circj.CJ-14-0840

All rights are reserved to the Japanese Circulation Society. For permissions, please e-mail: cj@j-circ.or.jp

(APN) is an adipokine with strong anti-inflammatory properties and has been suggested to play a protective role in the acute phase of myocarditis in humans.^{4,5} Importantly, it has been known that APN is downregulated in a variety of clinical conditions or critical illnesses, such as obesity, type 2 diabetes, and coronary artery disease.⁶ In addition, hepatocyte growth factor (HGF), another known anti-inflammatory adipokine, was reported to induce immune tolerance and functional recovery by use of an *in vivo* transfection technique in experimental autoimmune myocarditis (EAM).^{7,8} However, no clinically relevant method for the efficient delivery of APN or HGF into the heart has been well established for treating fulminant myocarditis.

We previously developed the epicardial transplantation of scaffold-free-induced adipocyte cell-sheet (iACS) method, and recently showed that iACS can constitutively deliver a variety of cardioprotective factors, including APN and HGF, to the heart in mice subjected to acute myocardial infarction.⁹ Importantly, iACS is generated from adipose tissue-derived stromal vascular fraction (SVF) cells that are isolated from the subcutaneous fat tissue without gene modification, which is promising for the potential use of this method in clinical settings.

We hypothesized that iACS transplantation into the heart might induce immune tolerance and functional recovery in autoimmune-associated myocarditis. Here we examined the biological and functional effects of this method as a drug-delivery system using an EAM rat model. Immunoinhibitory effects of pivotal paracrine factors, such as APN and HGF, on dendritic and effector T cells were also analyzed *in vivo* and *in vitro*. In addition, we generated a non-differentiating SVF cell-sheet (SVFCS) and showed that both the iACS and SVFCS produce a similarly great amount of anti-inflammatory adipokines, including HGF; however, differentiated iACS but not SVFCS was able to secrete a large amount of APN. Therefore, for the purpose of examining the additional effect of APN on EAM, we compared the therapeutic effects of iACS implantation with those of SVFCS implantation.

Methods

Animals

All animal studies were carried out under approval of the institutional ethics committee. This investigation conforms to the Principles of Laboratory Animal Care formulated by the National Society for Medical Research and the Guide for the Care and Use of Laboratory Animals (US National Institutes of Health Publication No. 85-23, revised 1996).

Preparation of SVFCS and iACS

Each iACS was prepared as previously described.⁹ Briefly, SVF cells isolated from inguinal adipose tissue were cultured on 35-mm thermo-responsive dishes (CellSeed, Tokyo, Japan), at 2×10^6 cells per dish, to generate each scaffold-free SVFCS. Each iACS was generated by adding 10 mg/ml insulin, 2 mmol/L dexamethasone, 5 mmol/L pioglitazone, and 125 mmol/L isobutylmethylxanthine (Sigma-Aldrich, St Louis, MO, USA) to the SVFCS for 2 days. The medium was then refreshed and the cultures incubated for 5 more days at 37°C. The iACS spontaneously detached from the surface when placed in a 20°C refrigerator.

Generation of the Rat Myocarditis Model and Cell-Sheet Transplantation

Purified porcine cardiac myosin (Sigma-Aldrich) was dis-

solved in 0.01 mol/L phosphate-buffered saline and emulsified with an equal volume of complete Freund's adjuvant (Difco Laboratories, Detroit, MI, USA). On days 0 and 7, 0.2 ml of the emulsion, which yielded an immunizing dose of 1.0 mg cardiac myosin per rat, was injected subcutaneously into the footpad of male Lewis rats (7 weeks old, 200–250 g).² Following the second injection, the rats were randomly assigned to 3 groups and subjected to a thoracotomy and: (1) a sham operation (Sham group; n=58) or transplantation onto the anterior surface of the heart of; (2) 3-layered SVFCS (SVFCS group; n=54); or (3) 3-layered iACS (iACS group; n=58).

Echocardiography and Conductance Catheter

Serial transthoracic echocardiography was performed under inhaled anesthesia with isoflurane (1.5%, 1 L/min; Mylan, Pittsburgh, PA, USA). Two-dimensional short-axis images at the basal, mid, and apical levels were acquired to calculate the left ventricular (LV) ejection fraction (EF) and regional wall motion index (RWMI).¹⁰

Pressure-volume (P-V) cardiac catheterization was performed after median sternotomy, by inserting a conductance catheter (Unique Medical, Tokyo, Japan) and a Micro Tip catheter transducer (SPR-671; Millar Instrument, Houston, TX, USA) into the LV cavity. The P-V loop data under stable hemodynamics or inferior vena cava occlusion were analyzed with Integral 3 software (Unique Medical).

CD4-Positive T-Cell Proliferation Assay

CD4-positive T cells and antigen-presenting dendritic cells were isolated from the spleen of EAM and normal rats, respectively, using magnetic-bead systems (Miltenyi Biotec, Bergish Gladbach, Germany). The isolated CD4-positive T cells and antigen-presenting dendritic cells were co-cultured in RPMI 1640 (Gibco, Grand Island, NY, USA) and 10% fetal bovine serum (FBS), supplemented with iACS supernatant, recombinant APN (Adipo Bioscience, CA, USA), or recombinant HGF (Institute of Immunology, Tokyo, Japan) for 5 days. Subsequently, 50 µg/ml purified porcine heart myosin was added, and T-cell proliferation was estimated using the Cell Counting Kit-8 (Dojindo, Kumamoto, Japan).⁸

Histology

Myocarditis severity was graded on hematoxylin and eosin (H&E)-stained whole sections (0, no inflammatory infiltrates; 1, small foci of inflammatory cells; 2, larger foci <100 inflammatory cells; 3, more than 10% of a cross-section involved; and 4, more than 30% of a cross-section involved).¹¹ The CD68-, CD4-, or CD4/Foxp3-positive cells were counted in 5 random fields (magnification: $\times 600$) to assess the infiltration of macrophages, CD4-positive T cells, or Foxp3-positive regulatory T cells, respectively.⁸

Statistical Analysis

Values are given as the mean \pm SD. All analyses were performed using SPSS 11.0J for Windows (SPSS, Chicago, IL, USA) and the R program.

Detailed methods are presented in **Supplementary File 1**.⁹

Results

Characterization of SVFCS and iACS *In Vitro*

The characteristics and fundamental behavior of the SVFCS and iACS were compared histologically and biochemically *in vitro*. The cells in the SVFCS were confluent and spindle-shaped. The cells in iACS were similar but many contained a

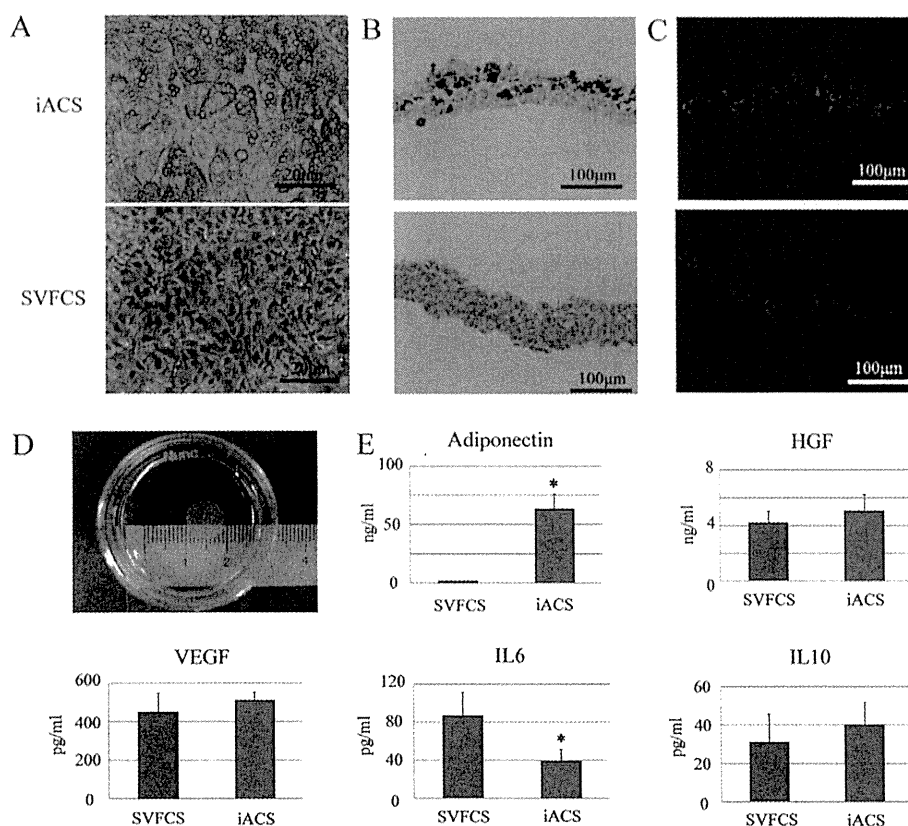


Figure 1. Characterization of the induced adipocyte cell sheet (iACS) in vitro. (A) Representative micrographs (B) Oil-red O staining. (C) Representative immunostaining for adiponectin (APN). Red indicates APN; blue, nuclei (n=7 each). (D) iACS detached from the temperature-responsive culture dish. (E) APN, hepatocyte growth factor (HGF), vascular endothelial growth factor (VEGF), interleukin (IL)6, and IL10 cytokine levels in cell-sheet supernatants by ELISA analysis (n=7 each). *P<0.05 vs. stromal vascular fraction cell-sheet (SVFCS). There was significantly more released APN in the culture supernatant of iACS than of SVFCS (P<0.001, unpaired t-test).

number of small cytoplasmic vesicles (Figure 1A) that stained positive with oil-red O, indicating that the vesicles were fat droplets. Only approximately half the SVF cells had differentiated into adipocytes (Figure 1B). Each iACS was approximately 9 mm in diameter and 140- μ m thick (Figure 1D). Immunohistolabeling revealed that APN was markedly upregulated in the cytoplasm of mature adipocytes in the iACS, but not in the undifferentiated SVF cells in the SVFCS (Figure 1C). The amount of extracellularly released APN in vitro was significantly and markedly greater in the culture supernatant of the iACS than in that of the SVFCS (P<0.001), as assessed by enzyme-linked immunosorbent assay (ELISA) (Figure 1E). The levels of HGF, vascular endothelial growth factor (VEGF) and anti-inflammatory IL10 were not significantly different between the SVFCS and the iACS, whereas the level of pro-inflammatory IL6 in the iACS culture supernatant was significantly lower (P=0.001).

Inhibition of Antigen-Specific CD4-Positive T-Cell Proliferation by iACS In Vitro

We first examined the expression of 2 different APN receptors (AdipoR1 and AdipoR2) in CD4-positive T cells, CD8-positive T cells and dendritic cells. Using quantitative real-time PCR, we detected similar levels of 2 genes in these 3 cell types

(Figure 2A).

Next, the effects of iACS transplantation on CD4-positive T-cell-related immunity in the EAM rats were assessed by an antigen-specific T-cell proliferation assay in vitro.

The addition of porcine myosin significantly and markedly increased the proliferation of CD4-positive T cells that were isolated from the spleen of the EAM rats (Figure 2B). The addition of recombinant APN and HGF at more than 30 ng/ml and 2 ng/ml, respectively, significantly suppressed the antigen-induced CD4-positive T-cell proliferation (Figure S1). The proliferation was diminished significantly more by the addition of an iACS supernatant, compared with 60 ng/ml APN or 5 ng/ml HGF, which were the average amounts released by iACS in vitro (P<0.001 for Myosin (+) vs. APN (60 ng/ml) and HGF (5 ng/ml vs. iACS supernatant). VEGF addition did not have any effect on T-cell proliferation (data not shown). ELISA analysis of the supernatant after incubating the antigen-induced CD4-positive T cells with a specific antigen revealed that adding recombinant APN (60 ng/ml), recombinant HGF (5 ng/ml) or iACS supernatant significantly diminished the release of IFN γ , IL17 and IL6 from the cells (Figures 2C–E).

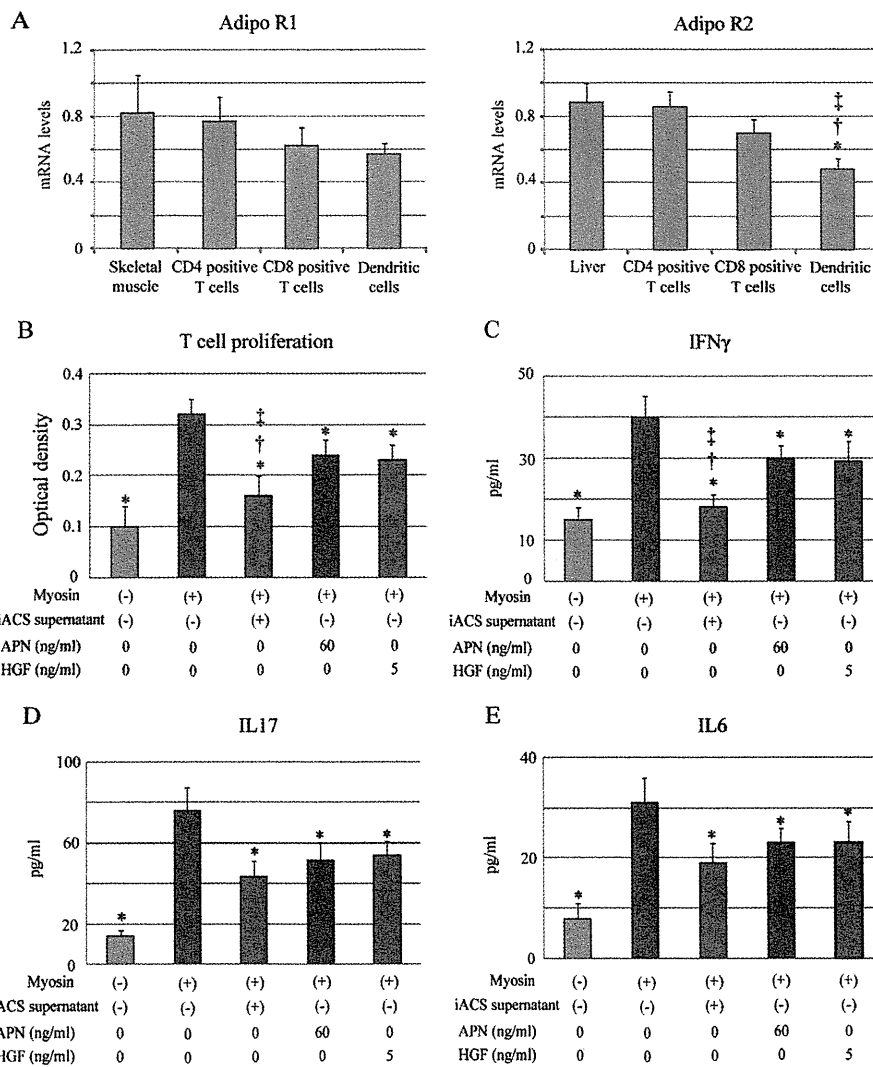


Figure 2. Expression of adiponectin (APN) receptors and CD4-positive T-cell proliferation assay. (A) mRNA levels of 2 different APN receptors (AdipoR1 and AdipoR2) in CD4-positive T cells, CD8-positive T cells and dendritic cells ($n=7$ each, ANOVA). * $P<0.05$ vs. Liver, † $P<0.05$ vs. CD4 positive T cells, # $P<0.05$ vs. CD8 positive T cells. All mRNA levels are normalized to GAPDH. (B–E) Addition of induced adipocyte cell-sheet (iACS) supernatant, recombinant APN (60ng/ml) or hepatocyte growth factor (HGF) (5 ng/ml) significantly suppressed the CD4-positive T-cell proliferation ($P<0.001$) and production of interferon (IFN) γ ($P<0.001$), interleukin (IL)17 ($P<0.001$) and IL6 ($P<0.001$) ($n=7$ each, ANOVA). * $P<0.05$ vs. Myosin (+), † $P<0.05$ vs. APN (60ng/ml), # $P<0.05$ vs. HGF (5ng/ml).

Delivery of APN, HGF and VEGF Into EAM Rat Heart by iACS Transplantation

The expression of APN, HGF and VEGF in the EAM rat heart after treatment was assessed by immunohistochemistry and ELISA. Most of the green fluorescent protein (GFP)-positive transplanted cells on day 21 in both the SVFCS and iACS groups remained on the surface of the heart (Figures 3B,C), and the number in both engrafted cell sheets gradually decreased from day 8 to day 42 (SVFCS: $P=0.026$, iACS: $P=0.045$; Figure 3J). Relatively small amounts of APN were detected at the inflamed interstitium and perivascular area in the Sham and SVFCS groups on day 21 (Figures 3A,B). In the iACS group, APN expression was higher at the interstitium near the inflammatory cells and the perivascular area,

especially in the epicardium near the transplanted iACS.

ELISA showed that the cardiac expression of APN in the inflamed area gradually increased over 42 days in the Sham and SVFCS groups, whereas the iACS transplantation significantly and markedly increased the APN expression compared to the other groups for 21 days; thereafter, high APN expression was maintained through the 42 days of the experiment (APN on day 21: $P=0.007$ for iACS vs. SVFCS and Sham; Figure 3G). Both HGF and VEGF were expressed in the inflamed area, but not in the non-inflamed area, on day 21 as assessed by immunohistochemistry (data not shown); the expression levels of HGF and VEGF on days 21 and 42 were similarly greater in the SVFCS and iACS groups than in the Sham group ([HGF on day 21: $P=0.001$ for iACS and SVFCS

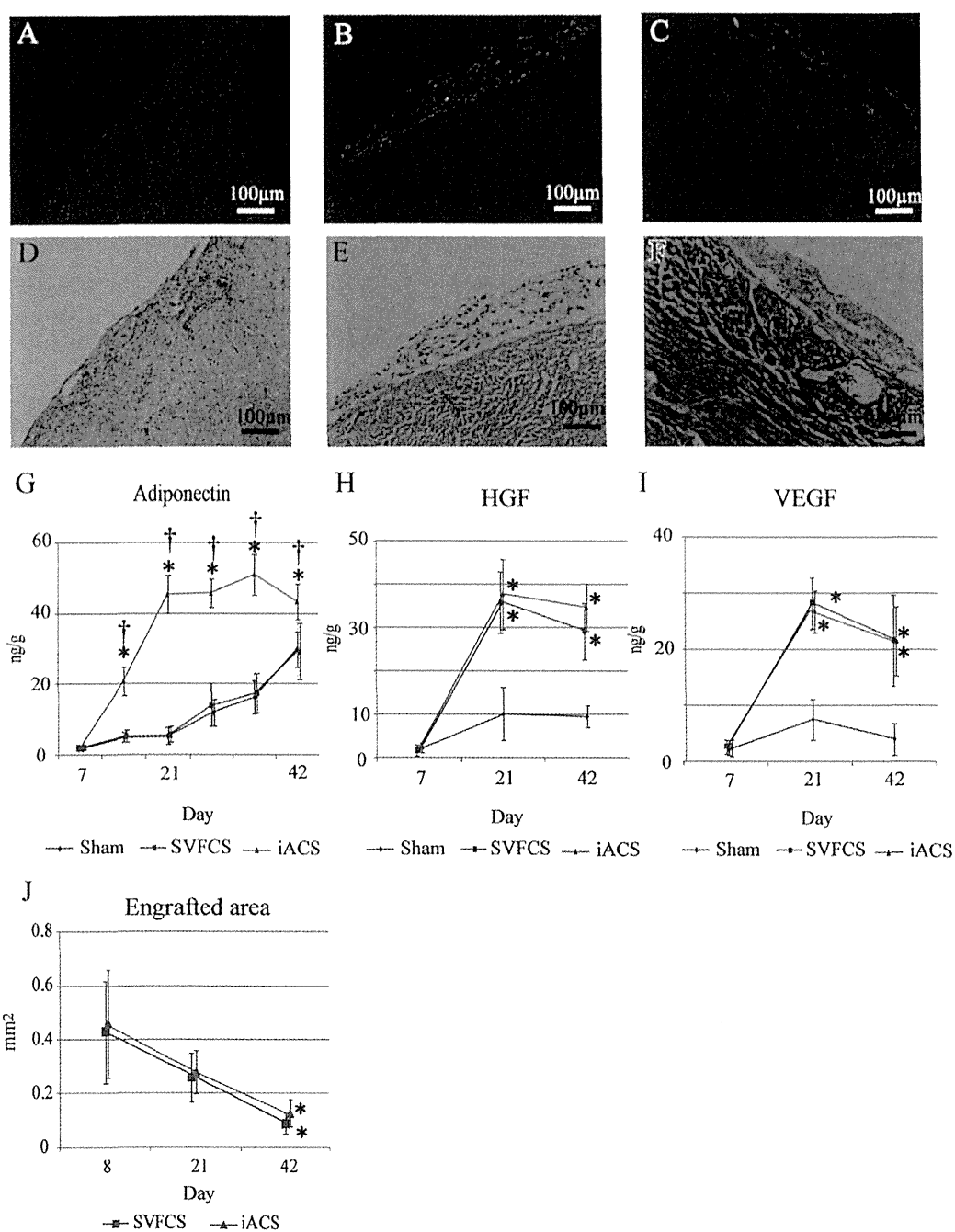


Figure 3. Delivery of cardioprotective factors to the experimental autoimmune myocarditis (EAM) rat heart by induced adipocyte cell-sheet (iACS) transplantation in vivo. (A–C) Representative immunostaining for adiponectin (APN) 14 days after the Sham operation (A), or green fluorescent protein (GFP)-positive stromal vascular-fraction cell-sheet (SVFCS) (B) and iACS (C) transplantation, respectively. Red, APN; blue, nuclei. (D–F) Hematoxylin and eosin staining of a serial section from the sample in (A), (B) and (C), respectively. (G–I) Cardiac expression of APN (G), hepatocyte growth factor (HGF) (H), and vascular endothelial growth factor (VEGF) (I) over time by ELISA (APN: Sham, n=7; SVFCS, n=6; iACS, n=7) (HGF and VEGF: Sham, n=6; SVFCS, n=5; iACS, n=7). *P<0.05 vs. Sham, †P<0.05 vs. SVFCS. (J), Quantification of the engrafted GFP-positive cell-sheet area in the iACS and SVFCS groups (n=4 each). *P<0.05 vs. day8.

vs. Sham] [VEGF on day 21: P<0.001 for iACS and SVFCS vs. Sham] (Figures 3H,I).

Induced ACS Transplantation Ameliorates Autoimmune Myocarditis in Rats

The severity of myocarditis in the EAM rats on day 21 was assessed and scored using H&E-stained heart sections (n=12